Size and composition dependence in the optical properties of mixed (transition metal/noble metal) embedded clusters

M. Gaudry, E. Cottancin,* M. Pellarin, J. Lermé, L. Arnaud, J. R. Huntzinger, J. L. Vialle, and M. Broyer
Laboratoire de Spectrométrie Ionique et Moléculaire, Université Claude Bernard Lyon I, UMR CNRS 5579, Bât. A. Kastler, 43 Bd. du 11 Novembre 1918, 69622 Villeurbanne Cedex, France

J. L. Rousset
Institut de Recherche sur la Catalyse, CNRS, 2 Av. Albert Einstein, 69626 Villeurbanne Cedex, France

M. Treilleux and P. Mélinon
Département de Physique des Matériaux, Université Claude Bernard Lyon I, UMR CNRS 5586, Bât. L. Brillouin, 43 Bd. du 11 Novembre 1918, 69622 Villeurbanne Cedex, France

(Received 8 November 2002; published 25 April 2003)

Optical properties of mixed clusters Ni/Ag, Co/Ag, and Ni/Au of 2–5 nm in diameter, produced by laser vaporization and embedded in an alumina matrix, are investigated. The first part is devoted to $(Ni_xAg_{1-x})_n$ clusters whose photoabsorption spectra reveal a surface plasmon resonance, damped, broadened, and blueshifted as compared to pure silver clusters. For a given mean size, a blueshift of the resonance band as well as a damping and broadening with increasing nickel proportion is observed, in good qualitative agreement with classical predictions, assuming a Ni-core/Ag-shell geometry. This core-shell structure is confirmed by low energy ion spectroscopy measurements showing that the cluster surface is essentially composed of silver. For a given composition, the size evolution of the plasmon band consists of a damping and broadening with decreasing size whereas no clear shift is noticed. Although the classical predictions, including the surface scattering limited mean free path contribution of the conduction electrons in the silver shell, account well for the size effects, inhomogeneous effects (size, shape, and local porosity) also contribute to the broadening and damping of the resonance in experiment. The second part concerns the optical properties of $(Co_{0.5}Ag_{0.5})_n$ and $(Ni_{0.5}Au_{0.5})_n$ clusters. The size evolution of the optical properties of $(Co_{0.5}Ag_{0.5})_n$ clusters is similar to that of $(Ni_{0.5}Ag_{0.5})_n$ clusters, with in addition, a weak blueshift of the resonance with decreasing size. As for the $(Ni_{0.5}Au_{0.5})_n$ clusters, their optical spectra do not display a marked resonance. The comparison with a core-shell model including a size dependent damping constant in the gold or silver shell gives a good understanding of these features for the two systems Co/Ag and Ni/Au.

DOI: 10.1103/PhysRevB.67.155409 PACS number(s): 36.40.Vz, 78.66.Bz, 78.67.−n

I. INTRODUCTION

The physics of nanoscaled systems or clusters has strongly developed in the last twenty years, and application outlooks appear to be more and more promising. For optical applications, clusters are also very attractive because their physical and chemical properties vary drastically with size.[1] From a fundamental point of view, their optical properties mirror their electronic structure and their geometry. For simple or noble metal clusters, the main feature of the optical response to excitation by light is an absorption band in the UV-visible range related to the surface plasmon resonance. Numerous studies have been performed on pure metal clusters such as alkali[2,3] or noble metals,[4–7] and the size dependence of their linear optical properties is now well understood.[8–10] New approaches are turned towards the dynamics or the nonlinear optical properties in such systems.[11,12] Another one is the study of mixed particles. From bulk metal physics, alloys are known to display original properties as compared to their constituents. Combining such distinctive features with those of clusters opens a new research field in the physics of nanoscaled systems.

In the nanometric scale, bimetallic clusters can form either alloys or segregated core-shell structures, depending on the properties of both components and on the production methods. As a rule of thumb, to minimize the total energy, one expects the component with the lower surface energy to accumulate preferentially at the surface. A model developed by Rousset *et al.*, based on a tight binding scheme, accounts well for the surface segregation observed in Pd/Pt clusters.[13,14] L. Yang *et al.*[15] drew the same conclusions for other bimetallic clusters, nevertheless the lattice mismatch between the two components may modify this empirical law. Moreover the phase diagrams of the alloys are also rich in information[16] to infer about the mixing of the two components of interest. Nevertheless, in the case of systems in solutions such as colloïds, one has to be careful with these simple rules because the kinetics of reduction may drive the final structure of the particles. Moreover, the surrounding medium and the surface adsorbed ions are also of main importance.[17] Much work was devoted to the optical properties of bimetallic particles, especially on the system Au/Ag (see the references listed in Ref. 18) or systems involving silver or gold. Among other works are those of Henglein *et al.* on core-shell systems such as Ag/Cd, Ag/Pb, Ag/In, and Au/Sb produced by chemical ways.[19–21] In all these systems in aqueous solution, the noble metal (Ag, Au) acts as an antenna for the other metal recovering it. For small deposits of the second metal, one can see a blueshift and a damping of

the noble metal plasmon resonance whereas the resonance band of the shell-metal clearly dominates the spectra (if it exists) for larger amounts of covering. In the case of Au/Sb, a competition between alloying and segregation seems to take place. Mixed noble metal clusters Au/Pt and Ag/Pt adsorbed on transparent immogolite fibers in aqueous solutions have been also investigated by Liz-Marzán *et al.*[22] Their method allows the preparation of bimetallic dispersions by simultaneous reduction of two bimetallic salts. The optical properties of these systems seem to show that the particles adopt a core-shell structure. The kinetics seem to play an important role in the process of formation of the clusters: the metal easier to reduce nucleates first and acts as a nucleation seed for the heteronucleation of the second metal. In this way, platinum surrounds silver or gold.

In most of the methods of production, it is difficult to vary independently the average size and composition of the nanoparticles. Moreover, alloyed structures are not easy to form. In contrast, it is possible to obtain core-shell structures for many systems which would spontaneously form an alloy under thermodynamical equilibrium conditions.

The codeposition of mixed clusters produced by laser vaporization technique with a continuous helium source permits variation of the size distribution of the clusters for a given stoichiometry. The size effects in mixed silver-gold clusters[23] with different proportions of gold have been previously studied and the results have shown that the electronic structure and the corresponding optical properties of the clusters embedded in alumina are consistent with an alloying structure.

As for mixed clusters containing nickel atoms, their optical properties have been seldom studied. A study on Cu/Ni clusters produced by ionic implantation in silica can be found in the literature.[24] The clusters form an alloy $Cu_{0.5}Ni_{0.5}$ but, as expected by the Mie theory, do not exhibit any plasmon resonance. To our knowledge, except for the low frequency Raman scattering experiment performed on our Ni/Ag cluster samples,[25] the Ni/Ag system has never been studied in the nanosized range. In the first instance, nickel and silver are known to be immiscible metals [see, for example, the phase diagram of Ni/Ag (Ref. 16)]. Much work on the evolution of Ni/Ag films with annealing shows that the nickel atoms bunch together to form seeds of pure nickel in a silver matrix.[26,27] Similar results have been obtained on Co/Ag films.[27] On the other hand, Ag/Ni alloy films prepared by simultaneous laser ablation of nickel and silver do not show any surface enhanced raman spectroscopy (SERS) activity directly after preparation.[28] After annealing or aging, the decomposition into two phases with Ag particles with very low Ni content and vice versa promotes the SERS enhancement (the influence of the transition metal vanishes). This effect might also be induced by segregation inside the particles. Anyhow, these studies show strikingly the high mobility of the atoms and the low interaction between Ag and Ni atoms. The results of the Raman spectrocopy lead to the same conclusions for the clusters. The acoustic mode frequencies of the Ni/Ag particles are in agreement with a core-shell structure for which the silver shell has a weak acoustic interaction with the nickel core. The observed quadrupolar mode corresponds nearly to the vibration of the silver shell alone.[25] Similar low frequency Raman scattering experiments have been performed on $(Co_{0.5}Ag_{0.5})_n$ clusters and the results are also consistent with a weak acoustic coupling between the cobalt core and the silver shell.[29]

Our study is devoted especially to the Ni/Ag sytem. In the present paper are detailed the nickel proportion dependence of the optical properties of the clusters and their size evolution for each composition. The experimental results are interpreted within a classical approach in the dipolar approximation (Mie theory). Results concerning $(Co_{0.5}Ag_{0.5})_n$ and $(Ni_{0.5}Au_{0.5})_n$ clusters are also reported and analyzed through classical descriptions assuming a core-shell geometry. Cobalt and nickel are metals with very similar properties and a complete study of the Co/Ag system seems unnecessary because it would probably be very close to the Ni/Ag one.

The plan of the paper is as follows. In Sec. II, we briefly review the experimental methods of elaboration and characterization of our samples. Low-energy ion spectroscopy (LEIS) measurements, giving information about the cluster surface composition, are largely discussed. Moreover an improvement of the absorption measurements performed under Brewster incidence is set out. We then provide the optical response obtained on mixed $(Ni_xAg_{1-x})_n$ clusters which are compared to classical models in Sec. III. We will see that the evolution of the optical properties with the sample aging can be understood by considering that the nickel weakly and progressively oxidizes. Section IV is devoted to the optical properties of $(Co_{0.5}Ag_{0.5})_n$ and $(Ni_{0.5}Au_{0.5})_n$ clusters.

II. EXPERIMENTS

A. Sample elaboration and characterization

Clusters are produced by a laser vaporization source (detailed in previous papers[4,30]) using a continuous flow of helium. The source works as follows: the second harmonic of a Nd: YAG pulsed laser (532 nm) is focused onto a metallic rod of the alloy A_xB_{1-x} to be studied in a small chamber under vacuum (A=Ni or Co, B=Ag or Au, and x is the atomic concentration of Ni or Co). The produced bimetallic plasma, cooled by the He gas, combines into clusters which expands with the inert gas through a nozzle. The so-formed clusters are then collimated with a skimmer into a high vacuum chamber (10^{-7}mbar) and codeposited with the transparent alumina matrix (evaporated thanks to an electron gun) on various substrates depending on the measurements to be performed. By varying the pressure between 20 and 60 mbar or by using a He-Ar mixture, one is able to change the mean size in our samples. Moreover, the metal volumic concentration in the sample is kept below 5% to minimize the cluster coalescence. The alumina matrix has an amorphous structure with a high porosity (45% compared to anodic alumina), is slightly overstoichiometric in oxygen ($Al_2O_{3.2}$), and transparent between 1 and 5.1 eV.[4] The typical nanocomposite samples then consist in a 1cm$\times$1cm square suprasil substrate of 1 mm thickness with about 200 nm of alumina doped with metal clusters.

The stoichiometry of the clusters has been probed through Rutherford back scattering (RBS) experiments. An He^+ ion

beam of 2 MeV in energy is focused on a cluster film deposited on silicon, and the analysis of the scattering energy of the He^+ ions, depending on the target elements *A* and *B*, permits us to obtain the relative abundances in the nanocomposite film. The measurements show that the relative atomic fraction A_xB_{1-x} of the target is recovered in all our samples to within $\Delta x/x = 5\%$. Furthermore, these results are confirmed by energy dispersive x-ray (EDX) experiments in which atoms, excited by electrons of an electron microscope, decay through x-ray emission whose analysis allows us to deduce the average composition of a cluster assembly under the electron beam. For instance, in the case of clusters produced from a target of an alloy $Ni_{0.5}Ag_{0.5}$, and from the examination of the nickel K_{α_1} and silver L_{α_1} emission rays, the average stoichiometry of $(Ni_xAg_{1-x})_n$ clusters is found to be $x = 50\% \pm 10\%$. Such results corroborate previous ones obtained on other bimetallic clusters produced by the laser vaporization technique for which the stoichiometry is always the same as that of the alloy target.[13,23]

The size distributions of the samples are determined from transmission electron microscopy (TEM). The TEM micrographs reveal almost spherical clusters randomly distributed in the transparent matrix. Size distributions are deduced from micrographs over populations of 300 to 1500 particles per sample. The size distributions follow a log-normal law with a standard deviation of about 40% of the mean diameter.

B. Low-energy ion spectroscopy experiments

From examination of bulk properties of nickel and silver, a likely cluster structure can be guessed. First, the atomic Wigner-Seitz radius of Ag and Ni are noticeably different, respectively, 3.02 and 2.6 a.u. (3.01 a.u. for gold and 2.6 a.u. for cobalt) and a pronounced lattice mismatch is expected. Second, the surface energy of silver is almost two times smaller than that of nickel. To minimize its energy, the composite system will have a majority of silver atoms on the surface. Furthermore, the phase diagram of Ni/Ag shows that silver and nickel are completely immiscible in any proportion. These basic properties strongly suggest that such a system will form a core-shell structure. The same hypothesis can be made for the Co/Ag particles.

In order to probe the surface composition of Ni/Ag clusters, we have performed LEIS experiments on $(Ni_{0.5}Ag_{0.5})_n$ clusters produced by our source and deposited on amorphous carbon under ultrahigh vacuum (10^{-10}mbar). The LEIS technique is the following: an $^4He^+$ ion beam of 1000 eV is directed onto the surface sample (spot of $0.1mm^2$) and one measures the kinetic energy distribution of the backscattered ions, function of the atomic mass of the target (elastic two-body scattering). During the bombardment, the cluster surface is progressively eroded. The evolution of the LEIS signal during the $^4He^+$ bombardment of the $(Ni_{0.5}Ag_{0.5})_n$ cluster sample after sputtering sequencies of 90, 345, 1290, and 3750 sec is displayed in Fig. 1. The signals corresponding to the masses of Ni and Ag are located around 790 and 885 eV, respectively. After a prior smoothing of the spectra, the peak areas which are proportional to the number of scattered atoms can be deduced. The scattering efficiency factors

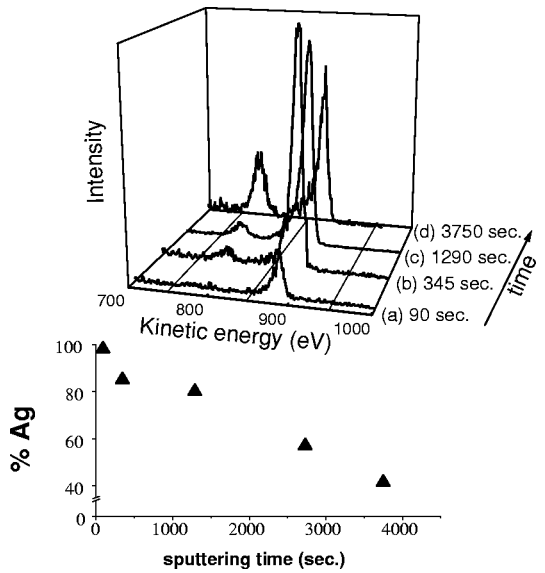

FIG. 1. Top: evolution of the whole LEIS spectra versus sputtering time for $(Ni_{0.5}Ag_{0.5})_n$ clusters; bottom: evolution of the silver concentration versus sputtering time.

f of Ni and Ag have been measured previously for an $^4He^+$ beam of 1 keV and their ratio $f_{Ag}/f_{Ni} = 2.52$. That means that the scattering cross section of silver is 2.52 times the one of nickel. From the ratio $I_{Ag}/(I_{Ag}+I_{Ni})$ one can deduce the cluster surface concentration whose evolution is plotted versus the sputtering time in the lower part of Fig. 1. At the very beginning of the sputtering, the signal reflects the cluster surface composition which is enriched in silver (95–100% of silver), confirming thus the segregation process. Then, the silver concentration decreases with sputtering time. This evolution originates from different effects. First, the erosion of the first atomic layer and second, the preferential erosion of silver as compared to nickel. We cannot gain more reliable information about the deeper layers since many dynamical processes come into play. For instance, intermixing and erosion by a local heating that can induce a diffusion of silver atoms towards the surface. Nevertheless, the main result is that the cluster surface is mostly composed of silver atoms. Combined with the immiscibility of the two metals, these results strongly suggest that the Ni/Ag system forms a core-shell structure, at least for a proportion of 50% of nickel.

C. Absorption measurements under Brewster incidence

Transmission measurements are performed with a Perkin-Elmer spectrophotometer in the energy range 1.55–6.52 eV (180–800 nm). In this range, the suprasil substrate is totally transparent but the transmission of alumina alone is progressively decreasing from about 4.5 eV to the UV domain. This feature is certainly due to light scattering owing to the granular structure of the porous matrix, and it partly blurs the intrinsic response of the embedded particles. To get rid of this spurious effect, the transmission spectra of the nanocomposite samples are normalized with the transmission spectra of pure alumina of about the same thickness and deposited on the silicon substrate. By concealing a part of the sample

from the cluster beam, it is possible to synthesize, at the same time, samples with two distinct regions: a first one covered with alumina doped with clusters and a second one covered only with alumina so as to serve as the reference for the normalization. The transmittance of the sample was previously recorded under normal incidence. The absorption coefficient is defined as $A=1-R-T$ where R is the reflectance. If R is neglected, the absorption coefficient is defined through the Beer-Lambert law $K_{\mathrm{abs}}=-\ln(T)/e$ where e is the film thickness of deposit. In fact, optical multilayers reflexion effects occur in our stratified samples and R can no longer be neglected. Oscillations in the transmission spectra are detected and are mainly due to corresponding oscillations in the reflectance R. Such oscillations have a period (of the order of 0.5 to 1 eV) inversely proportional to the film thickness and to the average optical indexes. A simple method for removing these oscillations from the absorption spectra is to use p-polarized light (the electromagnetic field $\vec{E}$ being in the incidence plane) under Brewster incidence (the Fresnel reflexion coefficient vanishes). The Brewster incidence Θ_B is connected with the average optical index of the pure alumina one $n_{\mathrm{Al_2O_3}}$ and $\tan\Theta_B=n_{\mathrm{Al_2O_3}}=1.64$ ($\Theta_B=58°$). We have tested the method on pure alumina films and the oscillations present under normal incidence almost completely vanish under Brewster incidence with p-polarized light.

This improvement in the absorption measurements does not call into question the previous results obtained on gold, silver, and gold-silver clusters but it is essential in the case of Ni/Ag clusters. Indeed the Fabry-Perot fringes may perturb the absorption measurements of the cluster sample, in particular when the resonance is strongly damped and broadened as observed in samples containing Ni/Ag clusters poor in silver. The real position of the resonance can be slightly shifted owing to these oscillations that can have close width and amplitude. Hence, for the most part, the results reported in the following have been performed under Brewster incidence with p-polarized light so that the absorption spectra reflect more confidently the absorption of the clusters in the sample. The use of a dichroic sheet polarizer restricts the measurement in the energy range 1.55–4.51 eV (275–800 nm).

III. OPTICAL PROPERTIES OF NI/AG CLUSTERS

A. Evolution with the composition

The $(\mathrm{Ni}_x\mathrm{Ag}_{1-x})_n$ mixed clusters have been investigated for different proportions of nickel ($x=0.0, 0.25, 0.5, 0.75, 1.0$). The evolution of the absorption spectra (obtained under Brewster incidence) versus the nickel proportion is displayed in Fig. 2(a). All the spectra correspond to samples characterized by almost the same optical diameter, namely, $D_{\mathrm{opt}}=\sqrt[3]{<D^3>}\simeq 2.6-2.7$ nm. The absorption spectrum of pure nickel clusters does not show any resonance band as predicted by the Mie theory when the dielectric function for the clusters is taken as the Ni bulk one. In contrast, for mixed $(\mathrm{Ni}_x\mathrm{Ag}_{1-x})_n$ clusters, a surface plasmon resonance is observed in the same spectral range as the one obtained for pure silver clusters but considerably

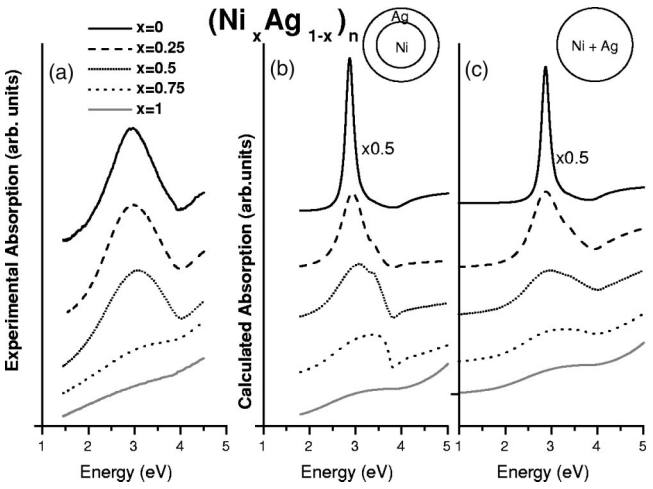

FIG. 2. Evolution of the optical absorption of Ni/Ag clusters with the nickel proportion for clusters with an optical diameter of about 2.6–2.7 nm. (a) Experimental absorption K_{abs}; (b) theoretical absorption $\sigma(\omega)$ within the classical core-shell model [Eq. (3)]. (c) Theoretical absorption $\sigma(\omega)$ for an alloyed homogeneous sphere with a dielectric function taken as the volumic composition weighted average of the dielectric functions of both component materials [Eq. (4)].

broadened. The resonance is clearly apparent when the proportion of silver exceeds 50%. Furthermore, a slight blueshift of the resonance is observed when increasing the nickel concentration from $x=0$ to $x=0.75$. This confirms the preliminary experimental results obtained under normal incidence.[31]

This experimental evolution has been compared to the one calculated within the extended Mie theory (i.e., more than one interface is involved) in the dipolar approximation. For that, let us recall that the absorption cross section in the dipolar approximation of a matrix-embedded metallic sphere subjected to an electromagnetic field is[32]

$$\sigma(\omega)=\frac{4\pi\omega}{c\varepsilon_m^{1/2}}\mathrm{Im}[\alpha(\omega)], \tag{1}$$

where $\alpha(\omega)$ is the polarizability of the particle, c the velocity of light, and ε_m the dielectric constant of the matrix. In the case of a homogeneous sphere of dielectric function ε and radius R,

$$\alpha(\omega)=\frac{\varepsilon-\varepsilon_m}{\varepsilon+2\varepsilon_m}\varepsilon_m R^3. \tag{2}$$

For a core-shell system such as Ni/Ag, the polarizability is

$$\alpha(\omega)=\frac{(\varepsilon_2-\varepsilon_m)(\varepsilon_1+2\varepsilon_2)+f_v(\varepsilon_1-\varepsilon_2)(\varepsilon_m+2\varepsilon_2)}{(\varepsilon_2+2\varepsilon_m)(\varepsilon_1+2\varepsilon_2)+2f_v(\varepsilon_2-\varepsilon_m)(\varepsilon_1-\varepsilon_2)}\varepsilon_m R^3. \tag{3}$$

ε_1 and ε_2 are, respectively, the complex dielectric functions of the core and shell bulk materials.[33] We will see in the following that the theoretical spectra exhibit discontinuities that can be attributed to the experimental data of the silver dielectric functions. The absorption spectrum of the core-shell particle depends on the volume ratio $f_v=(R_c/R)^3$ (R_c is the core radius and R the total radius of the particle). Using the atomic Wigner-Seitz radius of the core and shell materials, one can easily deduce the volumic ratio f_v for a given composition x. Calculations have been performed using the same total radius regardless of the composition and the dielectric constant of the matrix has been taken as the average experimental value $\varepsilon_m=2.7$. The theoretical results for a core-shell particle are reported in Fig. 2(b). The calculated absorption band is found to be larger than in the case of pure silver clusters, but it is still less important than the experimental broadening. It can be explained by the neglect of inhomogeneous effects in the samples (size, shape, and local porosity), but also by the use of the bulk dielectric functions of both materials which underestimate the damping constant Γ characterizing the conduction electron scattering rates in the particle. Nevertheless, the theoretical surface plasmon resonance is located in the same spectral range as the one obtained experimentally and the slight blueshift versus x is well reproduced by the core-shell model. The comparison with an alloyed homogeneous sphere whose dielectric function is described as an average of the component dielectric functions

$$\varepsilon=\varepsilon_{A_{x'}B_{1-x'}}(\omega)=x'\varepsilon_A(\omega)+(1-x')\varepsilon_B(\omega) \tag{4}$$

is also reported in Fig. 2(c). The volumic proportion x' of the material A is defined as

$$x'=\frac{1}{1+\dfrac{1-x}{x}\dfrac{r_s^3(B)}{r_s^3(A)}}, \tag{5}$$

where x is the atomic fraction of the material A.[34] One can see that the damping and broadening are more pronounced than those obtained with the core-shell model, and the position of the resonance is found to be redshifted as compared to the core-shell model and to experiment. In fact, the silver shell is not complete for clusters of 2.6 nm in diameter when the nickel proportion is larger than 46%, and thus it could be an explanation of the experimental damping for larger nickel proportions. Nevertheless, the broadening is also large for smaller nickel proportions in the clusters. The damping and broadening are among others due to a combination of inhomogeneous effects and the reduction of the electron mean free path in small clusters. Indeed, although the cluster size remains the same, the thickness of the silver shell is modified when the nickel proportion increases. Therefore, the influence of the reduction of the mean free path has been investigated in the framework of a simple model appropriate to a core-shell geometry. In this model the finite size effects are included by correcting the damping parameter Γ entering the Drude parametrization of the silver dielectric function associated to the conduction electron excitations. A similar correction cannot be carried out for nickel because its electronic band structure is more complex (*sp-d* band hybridization at the Fermi level). Owing to this severe shortcoming, only qualitative trends can be reasonably drawn from the simple model described below. The mean free path has been taken as proposed by Granqwist and Hunderi for a metallic sphere with a dielectric core (or equivalently a metallic shell)[35]

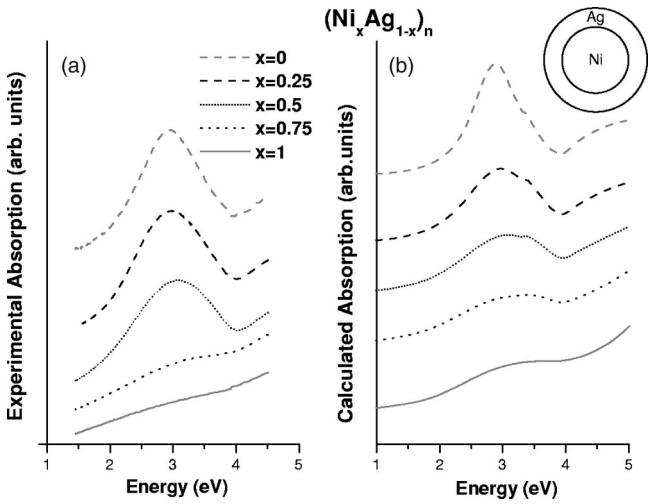

FIG. 3. comparison between experimental and theoretical absorption spectra of Ni/Ag clusters when the reduction of the mean free path in the silver shell is taken into account [Eqs. (7) and (3)].

$$l_{\text{path}}=\sqrt[3]{(R-R_c)(R^2-R_c^2)}. \tag{6}$$

In such a classical picture, the silver conduction electrons are assumed to be perfectly reflected from the Ni/Ag interface. The calculations have been also performed assuming a mean free path equal to the cluster radius R. The effective mean free path is probably between the two above values. Actually, both calculations lead to the same qualitative conclusions. To take into account the reduction of the mean free path of the silver conduction electrons the dielectric function has been corrected as follows:[1,36]

$$\varepsilon_2=\varepsilon_{\text{exp}}+\omega_p^2\left(\frac{1}{\omega^2+\Gamma_\infty^2}-\frac{1}{\omega^2+\Gamma_R^2}\right)+i\frac{\omega_p^2}{\omega}\left(\frac{\Gamma_R}{\omega^2+\Gamma_R^2}-\frac{\Gamma_\infty}{\omega^2+\Gamma_\infty^2}\right). \tag{7}$$

(ε_{exp}) is the bulk dielectric function of the shell and ω_p the plasma frequency (9 eV for silver), $\Gamma_\infty=0.021$ eV is the damping constant of bulk silver[37]and $\Gamma_R=\Gamma_\infty+Av_F/l_{\text{path}}$, the damping constant in the core-shell cluster. v_F denotes the Fermi velocity[38] and A is taken equal to 1 in our calculations. Let us emphasize that the above correction [Eq. (7)] depends implicitly on the assumption that the size dependence of the interband dielectric function of silver can be neglected in a first approximation.

Figure 3 shows that the experimental spectra are well reproduced by the model. The theoretical blueshift, damping, and widening with increasing proportion of nickel x reflect correctly the experimental trends. Indeed, for a given

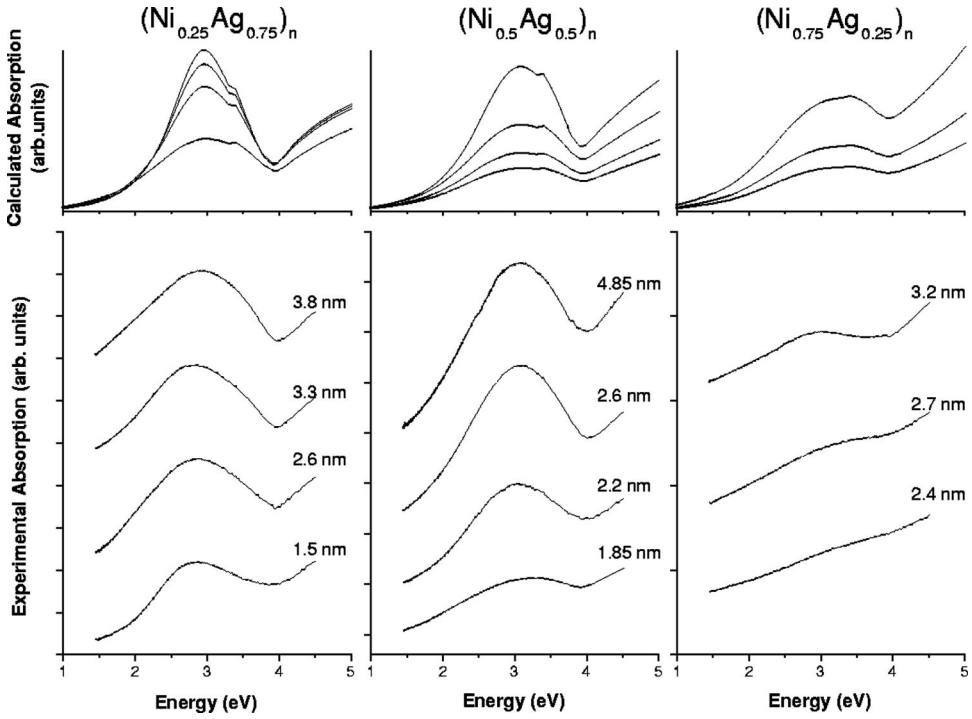

FIG. 4. Size evolution of the absorption spectra of Ni/Ag embedded clusters for each composition. Top: theoretical results within the core-shell model by taking into account the reduction of the mean free path in the silver shell. Bottom: experimental spectra under Brewster incidence except for $(Ni_{0.25}Ag_{0.75})_n$ for which the spectra have been recorded under normal incidence. The optical diameter is indicated for each spectrum.

size ($D=2.6$ nm in our case), the shell thickness decreases when the proportion of nickel increases, leading to an increase of the damping constant which varies from 0.725 eV for pure silver clusters to 2.23 eV for $(Ni_{0.75}Ag_{0.25})_n$ clusters. The real damping constant is probably smaller because inhomogeneous effects (size, shape, and local porosity) also contribute to the experimental broadening and damping.

Nevertheless, it must be emphasized that the model is very crude. Actually, for a small amount of silver ($x=0.75$), the silver shell is not complete (in particular for very small clusters) and the model is no longer realistic.

Finally, one can say that the experimental evolution of the absorption with the nickel proportion is intermediate between those of pure silver and pure nickel clusters. When increasing the nickel proportion in the clusters, the collective excitation of the conduction electrons in silver is more and more mixed with those involving the *sp-d* electrons in nickel, inducing the damping, broadening, and blueshift of the resonance. Their optical properties remain related to those of the pure constituents indicating that the dielectric function of the mixed Ni/Ag system and those of nickel and silver are closely correlated.

B. Evolution with the size

The size effects in the optical properties have been also investigated for each composition $x=0.25$, 0.5, and 0.75 and the corresponding absorption spectra are reported in the lower part of Fig. 4. The optical diameter is indicated for each spectrum. In the case of $(Ni_{0.25}Ag_{0.75})_n$ clusters, the spectra have been performed under normal incidence, but the resonance signal is strong enough and much larger than the Fabry-Perot fringes. One can suppose that the results under Brewster incidence would not have been noticeably modified. The main feature in the size evolution is the widening and damping of the resonance band with decreasing size. On the other hand, there is no evidence of a shift of the resonance. For $(Ni_{0.25}Ag_{0.75})_n$ clusters of 1.5 nm in diameter, the resonance band is thinner than for the other sizes. This is explained by the fact that the corresponding sample has been made on a substrate cooled to liquid nitrogen temperature. The corresponding size distribution is narrower under such conditions and that is thought to reduce cluster coalescence during the film growth. So, for this sample, a reduction of the inhomogeneous effects related to the size and shape of the clusters is expected. Indeed the coalescence being reduced, the tail of the distribution towards the large sizes is shortened and more clusters remain spherical.

The size effects are governed by many physical effects such as the electron spillout, the reduction of the screening at the cluster surface, and the local porosity at the cluster-matrix interface. One can imagine a model in which the Ni core should be classically treated through its experimental bulklike dielectric function and the Ag shell in a semiclassical way as previously described.[39] The *s*-silver electrons would be quantum mechanically treated, the ionic background as well as the surrounding matrix phenomenologically described by their respective bulk dielectric functions $\varepsilon_d(\omega)$ and $\varepsilon_m(\omega)$. The reduced screening at the shell surface would be mimicked by an inner skin of reduced polarizability and the local porosity by a cluster/matrix interface. The consistence of such a model where the silver shell is described subtly and the nickel core only by its bulk dielectric function would be questionable. This is why only a simple classical model has been used to interpret our results and why only qualitative information can be extracted. In the upper part of Fig. 4 are reported the theoretical absorption spectra of the clusters with sizes corresponding to the experimental ones. One can see that there is a good agreement

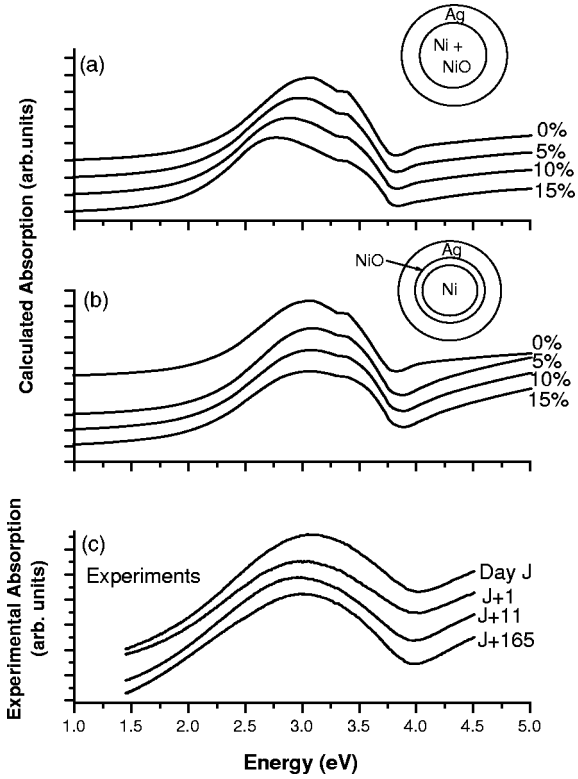

FIG. 5. Time evolution of the absorption spectra under Brewster incidence of $(Ni_{0.5}Ag_{0.5})_n$ clusters. Bottom: Experimental spectra. Top and middle: theoretical evolution of the absorption spectra with the nickel oxidation.

between experiment and theory. The damping and broadening are well reproduced if one takes into account the size dependent damping constant in the Drude component of the silver dielectric function. In the case of $(Ni_{0.75}Ag_{0.25})_n$ clusters, the resonance band is strongly attenuated, much more than the theoretical predictions. These results show the limits of the model when the clusters are very small or when the silver amount is not sufficient to form a monolayer at the surface.

C. Evolution of the samples with time

The time evolution of the optical spectra for $(Ni_{0.5}Ag_{0.5})_n$ clusters is given in Fig. 5(c). The main features in the spectra are a slight redshift of the resonance band and a weak damping with time. This evolution seems to occur merely during the first few days after the sample preparation, and to saturate thereafter. A similar evolution has been observed for the other compositions $x=0.25$ and $x=0.75$ but in the case of $x=0.25$, it is slower and weaker. The same aging effect has been observed in $(Co_{0.5}Ag_{0.5})_n$ clusters. The oxidation of the nickel or cobalt is suspected to induce such an evolution. Low frequency Raman spectroscopy experiments carried out on these samples containing $(Ni_xAg_{1-x})_n$ and $(Co_{0.5}Ag_{0.5})_n$ clusters do show peaks that can be assigned to nickel or cobalt oxide. The oxygen may penetrate the silver shell or bind with nickel or cobalt atoms which are still present at the surface. For $(Co_{0.5}Ag_{0.5})_n$ clusters, two peaks at 485 and 690 cm^{-1} have been identified corresponding to CoO bands. For Ni/Ag clusters, similar bands were observed but a bit less pronounced.[25,29,40] In contrast, similar bands corresponding to AgO have never been observed in pure silver clusters. We could also suppose that this oxidation induces a total separation of nickel and silver into partially oxidized nickel and silver nanoparticles. This phenomenom has already been observed in Ni-Al colloïds for which artificial oxidation leads to the formation of small nickel clusters isolated in aluminum oxide.[41] The nickel and silver, known to be immiscible, could also follow this way of separation. However, if it had been the case, the observed acoustic frequencies would have been higher and the surface plasmon resonance observed in absorption spectra would have been redshifted. In order to accelerate the oxidation, the sample was annealed at 80 °C during 6 h, but the absorption spectra remained unchanged. Then the sample was heated at 200 °C for 12 h. The corresponding spectra are then considerably damped but they are still large and do not correspond to the one of pure silver clusters. So we can reasonably conclude that the oxidation does not induce a separation of the Ni/Ag system. For clusters with a small amount of silver the oxidation occurs probably on the surface atoms of nickel preferentially.

To understand the role of the nickel oxidation in the evolution of the absorption spectra with time, two simple models are suggested. In the first one, the nickel oxide is assumed to form a thin layer [Fig. 5(b)] between the nickel core and the silver shell. The absorption has been calculated with this geometry[32] using the experimental bulk dielectric function of Ni, NiO,[42] and Ag. Figure 5(b) depicts the evolution of the spectra versus the percentage of nickel oxidation and one can see that the experimental redshift is not reproduced by this model. In the second model, one supposes to have a mixture of Ni and NiO in the spherical core whose dielectric function is taken as the weighted average of the Ni and NiO dielectric functions. Figure 5(a) gives the evolution of the optical spectra in this case as a function of the nickel oxidation. The redshift and the resonance shape are better reproduced with the second hypothesis. Although these calculations are made in the framework of a classical model and the oxidation is probably more complex, one can reasonably conclude that the oxidation remains weak (of about 5% after a few days and between 5 and 10 % after a few months). The aging of the samples has been studied for different compositions of Ni/Ag clusters and for Co/Ag clusters. It shows almost the same evolution whatever the cluster size is, for a given composition, and is all the more important that the nickel proportion is great. Concerning the stoichiometric effects (see Fig. 1), they have been performed just after the elaboration of the samples, so without oxidation. Moreover, the composition evolution in the optical absorption spectra, performed on samples of aging of about one year, are similar to those performed on fresh ones. The only difference rests in the absolute position of the resonance peaks which is redshifted.

For the size dependence evolution in the optical properties of $(Ni_xAg_{1-x})_n$ clusters, each range of size has been investigated with the same aging for each composition and in the case of $(Ni_{0.5}Ag_{0.5})_n$ clusters, the spectra have been performed on fresh samples. Therefore, the previous results are not disturbed by the oxidation. The only problem concerns

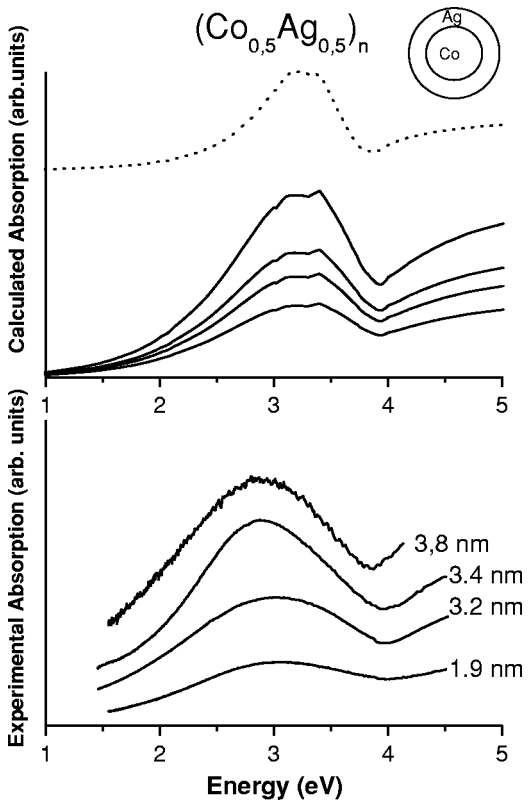

FIG. 6. Optical absorption in $(Co_{0.5}Ag_{0.5})_n$ clusters. Lower part: experimental spectra obtained under Brewster incidence. Upper part: core-shell model with experimental dielectric functions of Co and Ag (dotted line) and core-shell model by taking into account the reduction of the mean free path in the silver shell for the sizes corresponding to experiments (black line).

the redshift of the resonance with aging in $(Ni_{0.25}Ag_{0.75})_n$ and $(Ni_{0.75}Ag_{0.25})_n$ clusters. As the samples are of the same age for each composition, we can suppose that, for a given stoichiometry, the redshift is almost the same for each size. One can notice that for these two compositions the resonance is indeed redshifted compared to theory, all the more that the nickel proportion is important. In any case, the size evolution did not show any shift with decreasing size, so the size effects are not modified by sample aging.

IV. OPTICAL PROPERTIES OF CO/AG AND NI/AU CLUSTERS

A. The Co/Ag system

The optical properties of $(Co_{0.5}Ag_{0.5})_n$ clusters have been investigated in the size range 2.9–3.8 nm. Figure 6 gives a comparison between experimental and theoretical absorption spectra of different size distributions. The experimental evolution with decreasing size exhibits a strong broadening and damping but also a blueshift of the resonance. The interpretation of the magnitude of this shift has to be considered with caution because of the oxidation effects[29] (see Sec. III B). Nevertheless, since all the spectra have been recorded on samples with the same aging, this relative trend originates probably from finite-size effects. Within the classical core-shell model, the calculated spectrum (dotted line, Fig. 6) displays a narrower band compared to experimental spectra. By taking into account the reduction of the mean free path of the silver conduction electrons [Eq. (7)], a better agreement with experiment is obtained. Let us point out that the discontinuities in all the theoretical spectra (Fig. 6) can be attributed to the experimental tabulated data of the cobalt and silver dielectric functions.[33] One can see that the theoretical spectra are globally blueshifted compared to experimental ones. This difference is related to the oxidation which yields a redshift of the resonance. In return, regardless of the absolute position of the resonance peak, the evolution (damping and broadening) with decreasing size is well reproduced by the model.

Finally the optical properties of $(Co_{0.5}Ag_{0.5})_n$ clusters are quite close to those of $(Ni_{0.5}Ag_{0.5})_n$ clusters, except for the slight blueshift with decreasing size. With regard to the similarities of nickel and cobalt metals, the complete study for different stoichiometries would probably lead to the same conclusions.

B. The Ni/Au system

As with silver, gold is not miscible with nickel whatever the composition is, as illustrated by the Au-Ni phase diagram.[16] On the other hand, the difference between the surface energies of Ni and Au leads us to think that the nanoparticles will form a core-shell structure similar to the system Ni/Ag, but with a gold shell. Monte Carlo simulations support this assumption.[43] LEIS technique has been used for probing the surface composition of $(Ni_{0.5}Au_{0.5})_n$ clusters produced in the laser vaporization source and the results prove that the surface is entirely covered by gold atoms. X-ray photoemission experiments give the same conclusion concerning the segregation.[43] Samples of mixed $(Ni_{0.5}Au_{0.5})_n$ clusters embedded in alumina have been prepared. In order to vary the size distribution, the clusters have been deposited on silica substrates kept at a constant temperature of 400 °C. This technique was supposed to increase the coalescence during the cluster deposition as it was observed in the case of Pt/Ag clusters,[44] but for clusters containing gold, it seems that this temperature cannot shift the size distribution. Two experimental absorption spectra of mixed $(Ni_{0.5}Au_{0.5})_n$ clusters are reported in the lower part of Fig. 7. The lower spectrum does not display any resonance whereas the second one shows a very damped resonance. The comparison with a straight line (dots) highlights this flattened band. The classical core-shell model using the experimental bulk dielectric functions of both components gives a resonance band at around 2.4 eV (dotted line in the upper part of Fig. 7) but it is very narrow compared to the one observed in $(Ni_{0.5}Ag_{0.5})_n$ clusters. Experimentally, this band is not observed. By taking into account the reduction of the mean free path of the conduction electrons in the gold shell, the resonance band flattens out with decreasing size (upper part of Fig. 7). Bearing in mind that inhomogeneous effects induce also a damping and broadening of the plasmon band, the absence of a resonance in small clusters is finally not amazing. Actually, the plasmon resonance in pure gold

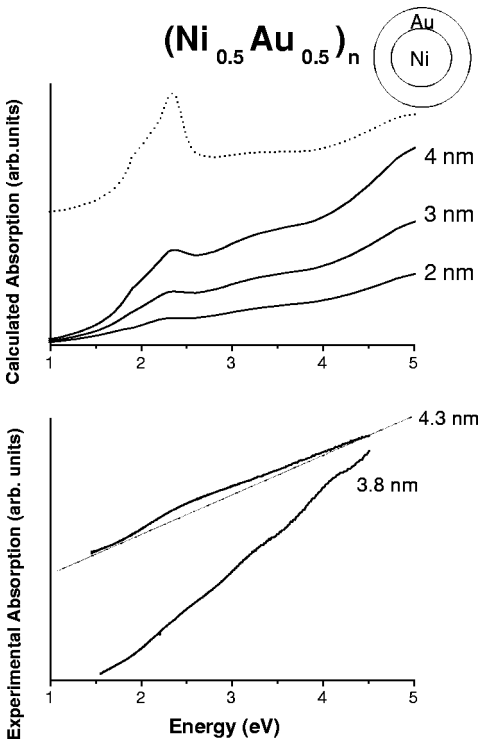

FIG. 7. Optical absorption in $(Ni_{0.5}Au_{0.5})_n$ clusters. Lower part: experimental spectra obtained under Brewster incidence for two different sizes. Upper part: core-shell model with experimental dielectric functions of Ni and Au (dotted line), core-shell model by taking into account the reduction of the mean free path in the gold shell for the indicating diameters (black line).

clusters is already above the threshold of the interband transitions. For Au/Ni clusters, the mixing with the electronic excitation in Ni probably smooths out the resonance in small clusters.

V. CONCLUSION

Linear optical properties of $(Ni_xAg_{1-x})_n$ clusters have been investigated. General considerations and LEIS experiments provided the undisputed evidence that the surface of the clusters is covered by silver atoms, suggesting that the geometry of the system is of core-shell type. The optical properties of this system were found to be intermediate between those of pure silver and pure nickel clusters, with a surface plasmon resonance enlarged and blueshifted compared to pure silver clusters. These features result from the mixing of the silver conduction electron collective excitation with those involving the nickel hybridized *sp-d* band electrons. The composition evolution as well as the size evolution of the optical properties are well understood within a classical core-shell model including the reduction of the conduction electron mean free path in the silver shell. However, this model seems to be inappropriate for small clusters poor in silver for which the silver shell cannot be complete. The Co/Ag system exhibits similar properties to the Ni/Ag one: a damping, widening and, in addition, a weak blueshift of the resonance with decreasing size, in good agreement with classical predictions. Its geometry can confidently be assumed to be the same as the Ni/Ag one with a cobalt core. The evolution of the spectra with time for Ni/Ag and Co/Ag clusters exhibits a redshift of the resonance band which has been explained by a weak oxidation of the nickel or cobalt atoms. Indeed, this evolution is well reproduced by a classical model involving an oxidized nickel core (or cobalt core). Finally, even if the Ni/Au system seems to be quite different in experiment, as no plasmon resonance is clearly characterized, it can be understood by the inhomogeneous effects and the reduction of conduction, electron mean free path in the gold shell.

Finally, one can say that the optical properties of these small mixed systems remain closely connected with the dielectric functions of their constituents. The size and stoichiometric effects are well understood through a classical description assuming a core-shell geometry and including the reduction of the valence electron mean free path in the silver or gold shell. Although these models are rather crude, especially for nanoscaled particles, they account well for the absorption spectra of the three studied systems. The agreement that is obtained in the three studied systems is perhaps rooted in a weak interaction between the core (Co, Ni) and shell (Ag, Au) atoms. One can also underline that it is essential to combine the study of the optical properties of clusters with LEIS experiments in order to determine the cluster structure.

ACKNOWLEDGMENTS

The authors are grateful to B. Prével and J. Tuaillon-Combes for Rutherford Back Scattering measurements. Many thanks to O. Boisron, A. Bourgey, C. Clavier, G. Guiraud, and F. Valadier for their essential technical support.

*Electronic address: cottanci@lasim.univ-lyon1.fr

[1] U. Kreibig and M. Vollmer, *Optical properties of metal clusters* (springer, Berlin, 1995).
[2] J. Blanc, V. Bonacic-Koutecky, M. Broyer, J. Chevaleyre, P. Dugourd, J. Koutecky, C. Scheuch, J. P. Wolf, and L. Wöste, J. Chem. Phys. **96**, 1793 (1992).
[3] C. Bréchignac, P. Cahuzac, N. Kebaïli, J. Leygnier, and A. Sarfati, Phys. Rev. Lett. **68**, 3916 (1992).
[4] B. Palpant, B. Prével, J. Lermé, E. Cottancin, M. Pellarin, M. Treilleux, A. Pérez, J. L. Vialle, and M. Broyer, Phys. Rev. B **57**, 1963 (1998).
[5] S. Fedrigo, W. Harbich, and J. Buttet, Phys. Rev. B **47**, 10 706 (1993).
[6] J. Tiggesbäumker, L. Köller, K. H. Meiwes-Broer, and A. Liebsch, Phys. Rev. A **48**, R1749 (1993).
[7] M. Alvarez, J. Khoury, T. Schaaff, M. Shafigullin, I. Vezmar, and R. Whetten, J. Phys. Chem. B **101**, 3706 (1997).
[8] L. Serra and A. Rubio, Phys. Rev. Lett. **78**, 1428 (1997).
[9] J. Lermé, B. Palpant, B. Prével, E. Cottancin, M. Pellarin, M. Treilleux, A. Pérez, J. L. Vialle, and M. Broyer, Eur. Phys. J. D **4**, 95 (1998)
[10] J. Lermé, B. Palpant, B. Prével, M. Pellarin, M. Treilleux, A.

Pérez, J. L. Vialle, and M. Broyer, Phys. Rev. Lett. **80**, 5105 (1998).
[11] C. Voisin, D. Christifilos, N. D. Fatti, F. Vallée, B. Prével, E. Cottancin, J. Lermé, M. Pellarin, and M. Broyer, Phys. Rev. Lett. **85**, 2200 (2000).
[12] N. Pincon, B. Palpant, D. Prot, E. Charron, and S. Debrus, Eur. Phys. J. D **19**, 395 (2002).
[13] J. Rousset, B. Khanra, A. Cadrot, F. C. S. Aires, A. Renouprez, and M. Pellarin, Surf. Sci. **352-354**, 583 (1996).
[14] J. Rousset, A. Renouprez, and A. Cadrot, Phys. Rev. B **58**, 2150 (1998).
[15] L. Yang, T. Raeker, and A. DePristo, Surf. Sci. **290**, 195 (1993).
[16] T. B. Massalski, J. L. Murray, L. H. Bernett, and H. Baker, *Binary Alloy Phase Diagrams (Vol 1 and 2)* (American Society for Metals, Metals Park, Ohio, 1986).
[17] P. Mulvaney, Langmuir **12**, 788 (1996).
[18] E. Cottancin, J. Lermé, M. Gaudry, M. Pellarin, J. L. Vialle, M. Broyer, B. Prével, M. Treilleux, and P. Mélinon, Phys. Rev. B **62**, 5179 (2000).
[19] A. Henglein, Ber. Bunsenges. Phys. Chem. **84**, 253 (1980).
[20] A. Henglein, P. Mulvaney, A. Holzwarth, T. Sosebee, and A. Fotjik, Ber. Bunsenges. Phys. Chem. **96**, 754 (1992).
[21] A. Henglein and M. Giersig, J. Phys. Chem. **98**, 6931 (1994).
[22] L. M. Liz-Marzan and A. P. Philipse, J. Phys. Chem. **99**, 15 120 (1995).
[23] M. Gaudry, J. Lermé, E. Cottancin, M. Pellarin, J. L. Vialle, M. Broyer, B. Prével, M. Treilleux, and P. Mélinon, Phys. Rev. B **64**, 085407 (2001).
[24] E. Cattaruzza, G. Battaglin, R. Polloni, T. Cesca, F. Gonella, G. Mattei, C. Maurizio, P. Mazzoldi, F. D. anf F. Zontone, and R. Bertoncello, Nucl. Instrum. Methods Phys. Res. B **148**, 1007 (1999).
[25] H. Portales, L. Saviot, E. Duval, M. Gaudry, E. Cottancin, M. Pellarin, J. Lermé, and M. Broyer, Phys. Rev. B **65**, 165422 (2002).
[26] O. Proux, J. Mimault, J. Regnard, C. Revenant, B. Mevel, and B. Dieny, J. Phys.: Condens. Matter **12**, 3939 (2000).
[27] O. Proux, J. Regnard, I. Manzini, C. Revenant, B. Rodmacq, and J. Mimault, Eur. Phys. J.: Appl. Phys. **9**, 115 (2000).
[28] E. Vogel and W. Kiefer, Asian J. Phys. **9**, 841 (2000).
[29] H. Portales, Ph.D. thesis, Université Claude Bernard Lyon 1, 2001.
[30] M. Pellarin, B. Baguenard, M. Broyer, J. Lermé, J. L. Vialle, and A. Pérez, J. Chem. Phys. **98**, 944 (1993).
[31] M. Gaudry, J. Lermé, E. Cottancin, M. Pellarin, B. Prével, M. Treilleux, P. Mélinon, J. L. Rousset, and M. Broyer, Eur. Phys. J. D **16**, 201 (2001).
[32] C. F. Bohren and D. P. Huffman, *Absorption and Scattering of Light by Small Particles* (Wiley, New York, 1983).
[33] E. D. Palik, *Handbook of Optical Constants of Solids* (Academic Press, New York, 1985), Vol. I; *Handbook of Optical Constants of Solids* (Academic Press, New York, 1991), Vol. II.
[34] The formula given for x' in Ref. 23 is an approximation suitable only if the Wigner-Seitz radii of both components are very close. In the case of Ni/Ag clusters, it is not the case and the exact formula has to be used.
[35] C. Granqwist and O. Hunderi, Z. Phys. B: Condens. Matter **30**, 47 (1978).
[36] H. Hövel, S. Fritz, A. Hilger, U. Kreibig, and M. Vollmer, Phys. Rev. B **48**, 18 178 (1993).
[37] P.B. Johnson and R. W. Christy, Phys. Rev. B **6**, 4370 (1972).
[38] C. Kittel, *Introduction to Solid State Physics* (Wiley, New York, 1983).
[39] J. Lermé, Eur. Phys. J. D **10**, 265 (2000).
[40] C. A. Melendres and S. Xu, J. Electrochem. Soc. Electrochem. Sci. Inst. **131**, 2239 (1984).
[41] O. Tillement, S. Illy-Cherrey, J. Dubois, S. Begin-Colin, F. Massicot, R. Schneider, Y. Fort, J. Ghanbaja, C. Bellouard, and E. Belin-Ferre, Philos. Mag. A **82**, 913 (2002).
[42] R. J. Powell and W. E. Spicer, Phys. Rev. B **2**, 2182 (1970).
[43] J. Rousset, F. C. S. Aires, B. Sekhar, P. Mélinon, B. Prével, and M. Pellarin, J. Phys. Chem. B **104**, 5430 (2000).
[44] E. Cottancin, M. Gaudry, M. Pellarin, J. Lermé, L. Arnaud, J. Huntzinger, J. Vialle, M. Treilleux, P. Mélinon, and M. Broyer, Eur. Phys. J. D (to be published).